Model-based analysis of polymer drag reduction in a turbulent channel flow

Binh K. Lieu and Mihailo R. Jovanović

Abstract— We develop a model-based approach for studying the influence of polymers on drag reduction in a turbulent channel flow. Our simulation-free method utilizes turbulence modeling in conjunction with the analysis of stochastically forced linearized equations to capture the effect of velocity and polymer stress fluctuations on the turbulent viscosity and drag. We demonstrate that the essential drag-reducing trends observed in high-fidelity numerical simulations are captured by our approach.

I. INTRODUCTION

The addition of a small amount of polymers to turbulent flows is an effective means for reducing skin-friction losses [1]. Most of our understanding on the onset of drag reduction and the interaction of polymers with turbulence comes from numerical and experimental studies. In particular, high-fidelity numerical simulations have offered tremendous insight on drag reduction mechanisms [2], [3], maximum drag reduction [4], and coherent structures [5]. In spite of this success, there is a need for the development of computationally attractive models that are suitable for analysis and identification of key physical mechanisms.

Study of polymer drag reduction is of both practical and fundamental importance. From applied point of view, the injection of high-molecular weight polymers to flowing liquids in pipe flows and marine vessels can have tremendous benefits. Polymer drag-reducing additives have been used in the Trans-Alaska Pipeline System to increase throughput and to maintain throughput with off-line pumping stations; polymer ejection has been used in US Navy submarine testings to reduce hull drag and increase speed by 10%–15% [1]. From fundamental point of view, understanding mechanisms of polymer drag reduction may shed light into the essential turbulent flow physics and open new ways of controlling turbulence via active or passive means.

In this paper, we combine turbulence modeling with analysis of stochastically forced linearized flow equations to quantify the polymer-induced drag reduction in a simulation-free manner. Our approach builds on recent efforts to develop model-based techniques for controlling the onset of turbulence [6], [7] and fully developed turbulent flows [8]. In contrast to the traditional approach that relies on numerical simulations, we use eddy-viscosity-enhanced linearization to determine influence of polymer additives on drag reduction. Our predictions capture the essential trends observed in numerical simulation studies.

B. K. Lieu and M. R. Jovanović are with the Department of Electrical and Computer Engineering, University of Minnesota, Minneapolis, MN 55455, USA (e-mails: lieux006@umn.edu, mihailo@umn.edu).
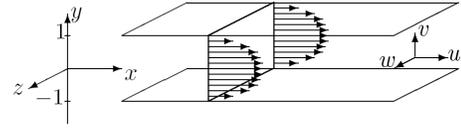

Fig. 1. Pressure driven channel flow.

Our presentation is organized as follows. In Section II, we formulate the problem and briefly discuss the governing equations and turbulence modeling. In Section III, we examine influence of fluctuations on the turbulent viscosity and drag using a stochastically forced model linearized around the approximation of the turbulent mean profile. We also present an efficient method for computing the second-order statistics of velocity and polymer stress fluctuations. In Section IV, we demonstrate that our model-based method is capable of predicting the essential drag-reducing trends. We conclude the paper with a brief summary of our developments and outlook for future research in Section V.

II. PROBLEM FORMULATION

We study a pressure-driven turbulent channel flow of a viscoelastic fluid in a Cartesian coordinate system (x, y, z) where x is the streamwise, y the wall-normal, and z the spanwise direction; see Fig. 1 for geometry. The conservation equations for momentum and mass are given by

$$\mathcal{U}_t = -(\mathcal{U} \cdot \boldsymbol{\nabla})\mathcal{U} - \boldsymbol{\nabla}\mathcal{P} + \frac{\beta}{R_\tau}\Delta \mathcal{U} + \frac{(1-\beta)}{R_\tau}\boldsymbol{\nabla} \cdot \mathcal{T},$$
$$0 = \boldsymbol{\nabla} \cdot \mathcal{U},$$

$$(1)$$

where $\mathcal{U}$ is the velocity vector, $\mathcal{P}$ is the pressure, $\mathcal{T}$ is the polymer stress tensor, $\boldsymbol{\nabla}$ is the gradient, and $\Delta = \boldsymbol{\nabla} \cdot \boldsymbol{\nabla}$ is the Laplacian. The Reynolds number $R_\tau = u_\tau h/\nu_0$ is defined in terms of the channel's half-height h, the friction velocity $u_\tau = \sqrt{(\tau_w/\rho)}$, and the zero shear rate kinematic viscosity $\nu_0 = \eta_0/\rho$ with τ_w being the wall-shear stress, ρ the fluid density, $\eta_0 = \eta_s + \eta_p$ the total viscosity, η_s and η_p the solvent and polymer viscosities. The parameter $\beta = \eta_s/\eta_0$ is the ratio of the solvent viscosity to the total viscosity; for $\beta = 1$ the fluid is Newtonian and (1) simplifies to the standard Navier-Stokes (NS) equations. System (1) has been brought to a non-dimensional form by scaling length with h, velocity with u_τ, time with h/u_τ, pressure with τ_w, and polymer stress with $\eta_p u_\tau/h$.

We describe the evolution of the polymer stress tensor $\boldsymbol{\tau}$

using the Oldroyd-B model,

$$\mathcal{T}_t = (1/We)\left(\boldsymbol{\nabla}\mathcal{U} + (\boldsymbol{\nabla}\mathcal{U})^T - \mathcal{T}\right) + \mathcal{T}\cdot\boldsymbol{\nabla}\mathcal{U} +$$
$$(\boldsymbol{\nabla}\mathcal{U})^T\cdot\mathcal{T} - (\mathcal{U}\cdot\boldsymbol{\nabla})\mathcal{T} + (D_0/R_\tau)\,\Delta\mathcal{T}. \quad (2)$$

The dimensionless parameter $We = \lambda u_\tau/h$ in (2) denotes the Weissenberg number which is defined as the ratio of the polymer relaxation time λ to the characteristic flow time h/u_τ. In turbulent flows, the friction Weissenberg number $We_\tau = \lambda u_\tau^2/\nu_0$ is typically used and the relationship between We and We_τ is given by

$$We = We_\tau/R_\tau.$$

The last term in (2) represents an artificial stress diffusive term. The numerical diffusivity is denoted by $D_0 = \kappa/\nu_0$ where κ is the isotropic numerical diffusivity. Addition of this term helps alleviate numerical instabilities associated with the standard Oldroyd-B model. For small D_0, [9] showed that artificial stress diffusivity has weak influence on the flow dynamics. In high-fidelity simulations of turbulent channel flows, D_0 is typically chosen to have the smallest value that provides numerically stable computations.

A. Equations for mean flow

Here, we present a method for computing an approximation of the mean turbulent velocity and polymer stresses. Even though this mean flow analysis shows that polymers reduce drag, it does not capture the essential drag-reducing trends observed in numerical simulations of the full-nonlinear equations. In Section III, we show that analysis of dynamics of flow fluctuations around this approximate mean flow improves predictive capability of our model-based approach.

The mean flow equations are obtained by splitting the flow quantities into their mean and fluctuating components

$$\mathcal{U} = \mathbf{U} + \mathbf{u}, \quad \mathcal{T} = \mathbf{T} + \boldsymbol{\tau}, \quad \mathcal{P} = P + p, \quad (3)$$

where $\mathbf{U} = \overline{\mathcal{U}}$, $\overline{\mathbf{u}} = 0$, with bar denoting averaging in time and horizontal directions. Substituting (3) into (1) and (2) and taking average in time and horizontal directions yield the steady-state mean equations for $\mathbf{U}$ and $\mathbf{T}$

$$0 = -(\mathbf{U}\cdot\boldsymbol{\nabla})\mathbf{U} - \nabla P + (\beta/R_\tau)\Delta\mathbf{U} +$$
$$((1-\beta)/R_\tau)\,\boldsymbol{\nabla}\cdot\mathbf{T} - \boldsymbol{\nabla}\cdot\left(\overline{\mathbf{u}\mathbf{u}^T}\right), \quad (4a)$$

$$0 = \boldsymbol{\nabla}\cdot\mathbf{U}, \quad (4b)$$

$$0 = (1/We)\left(\boldsymbol{\nabla}\mathbf{U} + (\boldsymbol{\nabla}\mathbf{U})^T - \mathbf{T}\right) + \mathbf{T}\cdot\boldsymbol{\nabla}\mathbf{U} +$$
$$(\boldsymbol{\nabla}\mathbf{U})^T\cdot\mathbf{T} - (\mathbf{U}\cdot\boldsymbol{\nabla})\mathbf{T} + (D_0/R_\tau)\Delta\mathbf{T} -$$
$$\overline{(\mathbf{u}\cdot\boldsymbol{\nabla})\boldsymbol{\tau}} + \overline{\boldsymbol{\tau}\cdot\boldsymbol{\nabla}\mathbf{u} + (\boldsymbol{\nabla}\mathbf{u})^T\cdot\boldsymbol{\tau}}. \quad (4c)$$

Since the second-order statistics of fluctuations are not known *a priori*, system (4) exhibits a closure problem. The first unknown term is the Reynolds stress tensor, $\overline{\mathbf{u}\mathbf{u}^T}$, which quantifies the transport of momentum arising from turbulent fluctuations. The remaining terms appear in the mean constitutive equation (4c),

$$\Gamma = \overline{(\mathbf{u}\cdot\boldsymbol{\nabla})\boldsymbol{\tau}}, \quad \Lambda = \overline{\boldsymbol{\tau}\cdot(\boldsymbol{\nabla}\mathbf{u}) + (\boldsymbol{\nabla}\mathbf{u})^T\cdot\boldsymbol{\tau}}, \quad (5)$$

where Γ represents the contribution to the transport of the polymer stress tensor arising from the fluctuating advective terms, and Λ accounts for the interactions between the fluctuating components of the polymer stress tensor and the velocity gradient tensor.

B. Turbulent eddy viscosity

One of the most commonly used models for the second-order statistics of velocity fluctuations is the Boussinesq approximation [10]

$$\overline{\mathbf{u}\mathbf{u}^T} = (2/3)\,k\,I - (\beta\nu_T/R_\tau)\left(\boldsymbol{\nabla}\mathbf{U} + (\boldsymbol{\nabla}\mathbf{U})^T\right), \quad (6)$$

where k is the turbulent kinetic energy, I is the identity operator, and ν_T is the turbulent eddy viscosity. In turbulent flows of viscoelastic fluids, ν_T is determined from statistics of velocity fluctuations and it is not known *a priori*. Hence, in order to accurately capture influence of velocity fluctuations on the turbulent mean velocity and polymer stresses we need an accurate model of ν_T. For Newtonian fluids, Reynolds & Tiederman [11] propose the following model for the turbulent eddy viscosity

$$\nu_{T0}(y) = \frac{1}{2}\left(\left(1 + \left(\frac{c_2}{3}\,R_\tau\,(1-y^2)\,(1+2y^2)\times\right.\right.\right.$$
$$\left.\left.\left.\times\,(1 - e^{-(1-|y|)\,R_\tau/c_1})\right)^2\right)^{1/2} - 1\right), \quad (7)$$

where c_1 and c_2 are modeling parameters selected to minimize least squares deviation between the mean streamwise velocity obtained with turbulent viscosity (7), and the mean streamwise velocity obtained in experiments and simulations. In particular, for simulation data of [12] at $R_\tau = 186$ we have $\{c_1 = 0.61, c_2 = 46.2\}$.

For flow subject to a constant pressure gradient $P_x = -1$, we determine an approximation to the mean turbulent profiles by neglecting the influence of fluctuations (5) in (4c) and utilizing (6) with eddy viscosity profile (7),

$$\mathbf{U} = \begin{bmatrix} U(y) \\ 0 \\ 0 \end{bmatrix}, \quad \mathbf{T} = \begin{bmatrix} T_{11}(y) & T_{12}(y) & 0 \\ T_{12}(y) & 0 & 0 \\ 0 & 0 & 0 \end{bmatrix}.$$

Homogeneous Dirichlet boundary conditions are imposed on U, and the boundary conditions for the polymer stresses are obtained using the procedure described in [9].

We next utilize perturbation analysis with $\alpha = 1 - \beta$ as the perturbation parameter to represent non-zero components of $\mathbf{U}$ and $\mathbf{T}$ as

$$U(y) = U_0(y) + \alpha\,U_1(y) + \mathcal{O}(\alpha^2),$$
$$T_{11}(y) = T_{11,0}(y) + \alpha\,T_{11,1}(y) + \mathcal{O}(\alpha^2),$$
$$T_{12}(y) = T_{12,0}(y) + \alpha\,T_{12,1}(y) + \mathcal{O}(\alpha^2).$$

By construction, U_0 approximates the mean streamwise velocity in the turbulent flow of Newtonian fluids. On the other hand, U_i, $T_{11,i}$, and $T_{12,i}$ for $i = 1, 2, \ldots$, denote
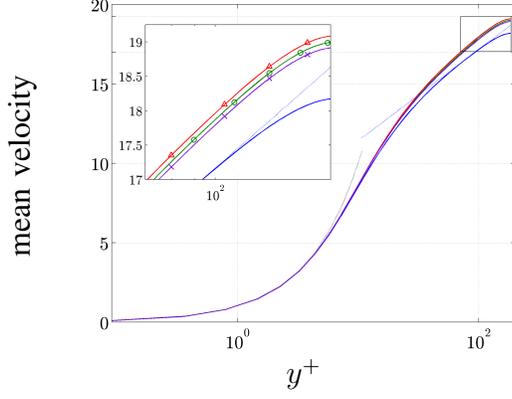
Fig. 2. Mean velocity as a function of the distance from the wall in flows with no polymers $U_0(y^+)$ (solid); and with polymers $U(y^+)$ for $We_\tau = 10$ ($\triangle$), $We_\tau = 50$ ($\circ$), and $We_\tau = 100$ ($\times$). For Newtonian fluids, we also show the linear wall asymptote, $U = y^+$, and the logarithmic inertial sublayer asymptote, $U = 2.5 \ln(y^+) + 6.5$. Results are obtained for flows with $R_\tau = 186$, $\beta = 0.9$, and $D_0 = 3.25$ using approximation up to fifth-order in α and the assumption that turbulent viscosity ν_{T0} captures the behavior of fluctuations.

corrections to U_0, $T_{11,0}$, and $T_{12,0}$ induced by polymers. They are obtained under the assumption that the turbulent viscosity is not modified by polymers and that the second-order statistics of fluctuations are not influencing the mean polymer stresses. Figure 2 shows the turbulent mean velocity profiles for the flow with no polymers U_0 and for the flow with polymers U as a function of the distance from the wall,

$$y^+ = R_\tau (y + 1).$$

As shown in figure 2, the linear relationship $U = y^+$ is satisfied in the viscous sublayer close to the wall ($y^+ < 2$). In the inertial sublayer far away from the wall ($y^+ > 50$), the Newtonian turbulent mean velocity is approximated by the logarithmic profile $U = 2.5 \ln(y^+) + 6.5$. This indicates that the turbulent mean profile computed using turbulent viscosity (7) captures the essential trends in turbulent flows with no polymers. In flows with polymers, U is increased in the inertial sublayer and the amount of increase is reduced as We_τ increases. We have used full-scale computations to verify the convergence of the perturbation series for the mean velocity and polymer stresses.

In flows with polymers, Housiadas & Beris [13] defined drag reduction as,

$$DR = 1 - (U_B/U_{B,0})^{-2/n}, \quad n = 1.14775, \quad (8)$$

where U_B and $U_{B,0}$ denote bulk velocities of flows with and without polymers,

$$U_B = \int_{-1}^{1} U(y) \, dy.$$

The mean velocity profiles shown in figure 2 induce 7.27%, 6.75%, and 5.77% of drag reduction at $We_\tau = 10$, 50, and 100, respectively. Although in all three cases drag reduction is achieved, decrease in drag reduction with We_τ contradicts high-fidelity numerical simulation trends [14]. This indicates

that the amount of drag reduction at large values of We_τ is not correctly predicted by the above mean flow analysis.

III. STOCHASTICALLY FORCED FLOW WITH POLYMERS: FLUCTUATION DYNAMICS

In this section, we examine the dynamics of infinitesimal velocity and polymer stress fluctuations around the mean flow $(\mathbf{U}, \mathbf{T})$ of Section II-B. Our model-based approach is similar to the method that Moarref & Jovanović [8] recently used to design drag-reducing transverse wall-oscillations. Our analysis utilizes the NS and constitutive equations linearized around the turbulent mean flow of Section II-B

$$\mathbf{u}_t = -(\mathbf{U} \cdot \boldsymbol{\nabla}) \mathbf{u} - (\mathbf{u} \cdot \boldsymbol{\nabla}) \mathbf{U} - \nabla p + \frac{\alpha}{R_\tau} \boldsymbol{\nabla} \cdot \boldsymbol{\tau} +$$

$$\frac{1 - \alpha}{R_\tau} \boldsymbol{\nabla} \cdot \left((1 + \nu_{T0}) \left(\boldsymbol{\nabla} \mathbf{u} + (\boldsymbol{\nabla} \mathbf{u})^T \right) \right), \quad (9a)$$

$$0 = \boldsymbol{\nabla} \cdot \mathbf{u}, \quad (9b)$$

$$\boldsymbol{\tau}_t = \frac{1}{We} \left(\boldsymbol{\nabla} \mathbf{u} + (\boldsymbol{\nabla} \mathbf{u})^T - \boldsymbol{\tau} \right) + \frac{D_0}{R_\tau} \Delta \boldsymbol{\tau} +$$

$$\mathbf{T} \cdot \boldsymbol{\nabla} \mathbf{u} + (\boldsymbol{\nabla} \mathbf{u})^T \cdot \mathbf{T} - (\mathbf{u} \cdot \boldsymbol{\nabla}) \mathbf{T} +$$

$$\boldsymbol{\tau} \cdot \boldsymbol{\nabla} \mathbf{U} + (\boldsymbol{\nabla} \mathbf{U})^T \cdot \boldsymbol{\tau} - (\mathbf{U} \cdot \boldsymbol{\nabla}) \boldsymbol{\tau}, \quad (9c)$$

where $\alpha = 1 - \beta$ and

$$\mathbf{u} = \begin{bmatrix} u \\ v \\ w \end{bmatrix}, \quad \boldsymbol{\tau} = \begin{bmatrix} \tau_{11} & \tau_{12} & \tau_{13} \\ \tau_{12} & \tau_{22} & \tau_{23} \\ \tau_{13} & \tau_{23} & \tau_{33} \end{bmatrix},$$

with τ_{ij} representing the fluctuating components of the polymer stress tensor and u, v, and w denoting the velocity fluctuations in the streamwise, wall-normal, and spanwise directions. The evolution form of (9) is obtained by eliminating the pressure from the equations, and by expressing the velocity fluctuations in terms of the the wall-normal velocity v and vorticity $\eta = \partial_z u - \partial_x w$. Furthermore, by rearranging the components of $\boldsymbol{\tau}$ and by applying the Fourier transforms in the x and z-directions we arrive at a set of PDEs in y and t parameterized by the wave-numbers $\boldsymbol{\kappa} = (k_x, k_z)$,

$$\boldsymbol{\psi}_t (y, \boldsymbol{\kappa}, t) = A(\boldsymbol{\kappa}) \boldsymbol{\psi} (y, \boldsymbol{\kappa}, t) + B(\boldsymbol{\kappa}) \mathbf{f} (y, \boldsymbol{\kappa}, t),$$
$$\boldsymbol{\phi} (y, \boldsymbol{\kappa}, t) = C(\boldsymbol{\kappa}) \boldsymbol{\psi} (y, \boldsymbol{\kappa}, t), \quad (10)$$

where $\boldsymbol{\psi} = \begin{bmatrix} \boldsymbol{\psi}_1^T & \boldsymbol{\psi}_2^T \end{bmatrix}^T$ is the state vector with

$$\boldsymbol{\psi}_1 = \begin{bmatrix} v & \eta \end{bmatrix}^T,$$
$$\boldsymbol{\psi}_2 = \begin{bmatrix} \tau_{22} & \tau_{23} & \tau_{33} & \tau_{12} & \tau_{13} & \tau_{11} \end{bmatrix}^T.$$

The output vector $\boldsymbol{\phi}$ contains the velocity and polymer stress fluctuations. Due to space constraints, the operators in (10) will be reported elsewhere. System (10) is forced with a zero-mean temporally white stochastic process $\mathbf{f}$,

$$\mathcal{E} (\mathbf{f} (\cdot, \boldsymbol{\kappa}, t_1) \otimes \mathbf{f} (\cdot, \boldsymbol{\kappa}, t_2)) = M(\boldsymbol{\kappa}) \delta(t_1 - t_2), \quad (11)$$

where δ is the Dirac delta function, $\mathbf{f} \otimes \mathbf{f}$ is the tensor product of $\mathbf{f}$ with itself, and $M(\boldsymbol{\kappa})$ is the spatial spectral-density of
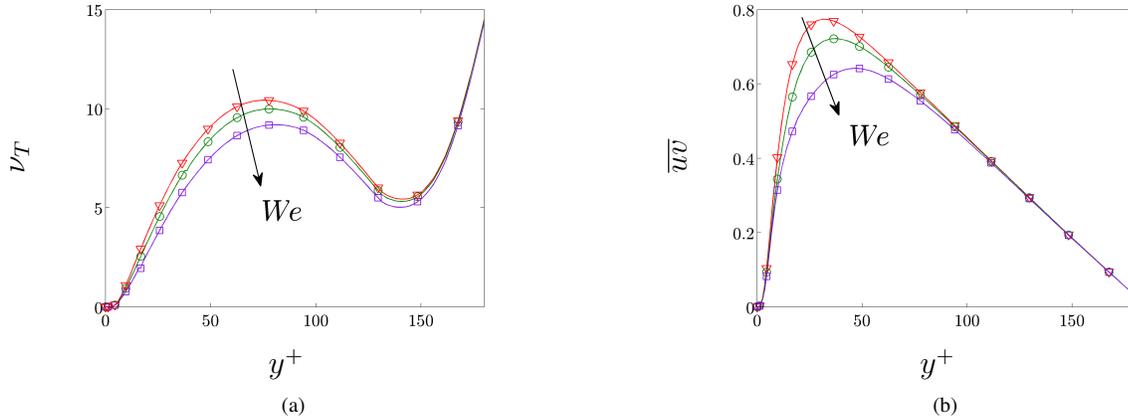
Fig. 3. (a) Turbulent eddy viscosity ν_T and (b) Reynolds stress $\overline{uv}$ as a function of y^+ for $R_\tau = 186$, $\beta = 0.9$, $D_0 = 3.25$: $We_\tau = 50$ ($\bigtriangledown$); $We_\tau = 70$ ($\circ$); and $We_\tau = 100$ ($\square$). Perturbation series up to fifth order in α with Shanks approximation is used to obtain ν_T and $\overline{uv}$.

the forcing.

Jovanović & Georgiou [15] showed that the steady-state statistics of velocity fluctuations in homogeneous isotropic turbulence can be reproduced by driving linearized NS equations with white-in-time forcing and properly selected spatial spectral-density. Inspired by this observation, Moarref & Jovanović [8] determined $M(\boldsymbol{\kappa})$ to match the simulation-generated energy spectrum in Newtonian turbulent channel flows. We adopt the model for spatial spectral-density of forcing developed in [8].

For the linearized system (10), the steady-state autocorrelation tensor of flow fluctuations is obtained by solving the Lyapunov equation [16]

$$A(\boldsymbol{\kappa})\,X(\boldsymbol{\kappa}) + X(\boldsymbol{\kappa})\,A^*(\boldsymbol{\kappa}) \;=\; -B(\boldsymbol{\kappa})\,M(\boldsymbol{\kappa})\,B^*(\boldsymbol{\kappa}), \quad (12)$$

where the asterisk denotes the adjoint of the corresponding operator. The operator X represents the autocorrelation operator of $\boldsymbol{\psi}$ and it contains all second-order statistics of velocity and polymer stress fluctuations. Furthermore, since we use a perturbation series to represent the mean velocity $\mathbf{U}$, the operator X can be represented as

$$X \;=\; X_0 + \alpha\,X_1 + \alpha^2\,X_2 + \mathcal{O}(\alpha^3), \quad (13)$$

where X_0 denotes the autocorrelation operator in the turbulent flow of Newtonian fluids, and X_i for $i = \{1, 2, 3, \ldots\}$ denote the corrections induced by polymers.

By selecting proper velocity and length scales, the eddy viscosity can be expressed as

$$\nu_T \;=\; C_\mu\,R_\tau^2\,\frac{k^2}{\epsilon}, \quad (14)$$

where ϵ is the rate of energy dissipation and $C_\mu = 0.09$ is a model constant. Here, we utilize the autocorrelation operator X to determine the second-order statistics of the velocity fluctuations and consequently k and ϵ. By expressing k and ϵ in terms of power series expansion (in α), ν_T can

be represented as

$$\begin{aligned}
\nu_T &= \nu_{T0} + \alpha\,\nu_{T1} + \mathcal{O}(\alpha^3), \\
\nu_{T1} &= \nu_{T0}\,(2\,k_1/k_0 - \epsilon_1/\epsilon_0),
\end{aligned} \quad (15)$$

where ν_{T0} is the Reynolds–Tiederman eddy viscosity profile (7).

The developments of this section are used to study the influence of polymers on the turbulent viscosity, mean velocity, drag, and turbulent kinetic energy; see Section IV for details.

IV. RESULTS AND DISCUSSIONS

In this section, we examine the effect of flow fluctuations on the eddy viscosity, turbulent mean velocity, drag, and turbulent kinetic energy in flows with $R_\tau = 186$, $\beta = 0.9$, and $D_0 = 3.25$. We also analyze how We_τ influences the drag-reducing trends and compare our predictions with simulation results of [4]. Furthermore, we study how polymers influence the energy amplification of turbulent velocity fluctuations.

We use perturbation analysis up to fifth order in α in all our computations. In addition, for each computed flow quantity a series acceleration method known as Shanks transformation [17] is used to increase the rate of convergence of the perturbation series. The finite-dimensional approximations of the underlying operators are obtained using the pseudospectral method [18]. An automatic Chebyshev collocation method [19] was also employed to verify our results.

A. Turbulent eddy viscosity and Reynolds shear stress

We first discuss the effect of polymers on the turbulent eddy viscosity ν_T and Reynolds shear stress $\overline{uv}$. Figure 3(a) shows the turbulent viscosity ν_T obtained using (14). The eddy viscosity increases from zero at the channel wall to a maximum value within the core of channel. As the friction Weissenberg number increases, ν_T decreases at all points in the channel. In flows with polymers, the Reynolds shear stress shown in Fig. 3(b) is computed using the second-order statistics of stochastically forced linearized equations.
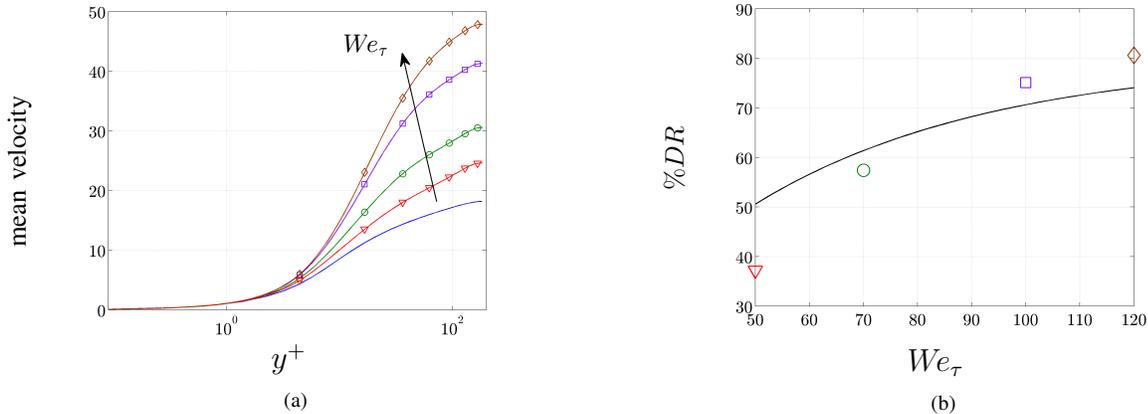
Fig. 4. Modified turbulent mean velocity and drag reduction computed using ν_T, Γ, and Λ for $R_\tau = 186$, $\beta = 0.9$, and $D_0 = 3.25$. (a) mean velocities with no polymers $U_0(y^+)$ (solid) and with polymers $U(y^+)$ for $We_\tau = 50$ ($\triangledown$), $We_\tau = 70$ ($\circ$), $We_\tau = 100$ ($\square$), and $We_\tau = 120$ ($\diamond$). (b) Drag reduction obtained using the mean velocities shown in (a). An approximation of the amount of drag reduction achieved in high-fidelity simulations of [4] is also shown in (b).

Similar to the eddy viscosity, the value of $\overline{uv}$ decreases throughout the channel as We_τ is increased. We note that reductions in the turbulent eddy viscosity and Reynolds shear stress indicate that the drag is reduced; see Section IV-B for additional details. Furthermore, the above-observed trends are in good agreement with the numerical findings of [4], [20].

B. Turbulent mean velocity and drag reduction

We next examine the influence of velocity and polymer stress fluctuations on the streamwise mean velocity and drag reduction. The modified turbulent mean velocity and polymer stresses are obtained by solving the equations for mean flow (4) – (6) with the corrected eddy viscosity (14). Note that the second-order statistics of flow fluctuations (5), Γ and Λ, are obtained from the autocorrelation operator X.

The modified turbulent mean velocity and drag reduction are shown in Fig. 4. Figure 4(a) demonstrates that the fluctuations around the base flow computed in Section II-B have profound influence on the turbulent mean flow; c.f. Figs. 2 and 4(a). For all mean velocities, the constant pressure gradient constraint induces a linear dependence on y^+ in the viscous sublayer close to the wall. As the friction Weissenberg number We_τ increases the streamwise velocity is increased in the inertial sublayer, which also increases the amount of drag reduction; see Fig. 4(b). Figure 4(b) also shows a curve that approximates the amount of drag reduction obtained in simulations of the nonlinear NS and FENE-P equations [4]. Although the amount of drag reduction computed using our simulation-free method does not match exactly the fitted curve, the drag-reducing trends as a function of We_τ are nicely captured. More interestingly, it appears that our method is capable of capturing the saturation of drag reduction at large We_τ. This phenomenon is known as the maximum drag reduction asymptote [1]. In our future work, we intend to gain additional insight into this phenomenon by conducting study of the drag reduction dependence on $1/We_\tau$ in flows with high We_τ.

C. Turbulent kinetic energy

Here, we study the energy amplification of velocity fluctuations in the flow with polymers. Up to the second order in α, we have

$$E(k_x, k_z) = E_0(k_x, k_z) + \alpha E_1(k_x, k_z) + \mathcal{O}\left(\alpha^2\right),$$
$$= E_0(k_x, k_z) + E_p(k_x, k_z),$$

where E_0 represents the energy spectrum of the flow with no polymers and E_p denotes the correction induced by polymers. The energy spectrum of the turbulent channel flow of Newtonian fluids E_0 is obtained by [12] and it is always positive. On the other hand, the corrections to it can assume both positive and negative values. Figure 5 shows the corrections to the pre-multiplied energy spectrum of the velocity fluctuations induced by polymers,

$$\mathcal{E}_p(k_x, k_z) = k_x\, k_z\, E_p(k_x, k_z).$$

In all three cases, the area under $\mathcal{E}_p$ is positive indicating that polymer additives increase the turbulent kinetic energy, which is in agreement with the simulation results of [3]. At $We_\tau = 50$, Fig. 5(a) shows energy amplification in the region where $k_x \sim \mathcal{O}(1)$ and $k_z \sim \mathcal{O}(1)$. As Weissenberg number increases, the largest amplification decreases. Furthermore, in all three cases, there is a narrow region of the wavenumbers where polymers slightly reduce fluctuations' energy; as We_τ increases, the amplitude in this region gets increased. This illustrates that energy amplification is reduced as the ratio of the polymer relaxation time to the characteristic flow time increases.

V. CONCLUDING REMARKS

We have developed a model-based approach for studying polymer drag reduction in a turbulent channel flow. Our simulation-free method provides a computationally-efficient way for predicting the amount of drag reduction by polymer additives. This is achieved by combining turbulent viscosity hypothesis with stochastically forced linearized flow equations to study the influence of infinitesimal fluctuations
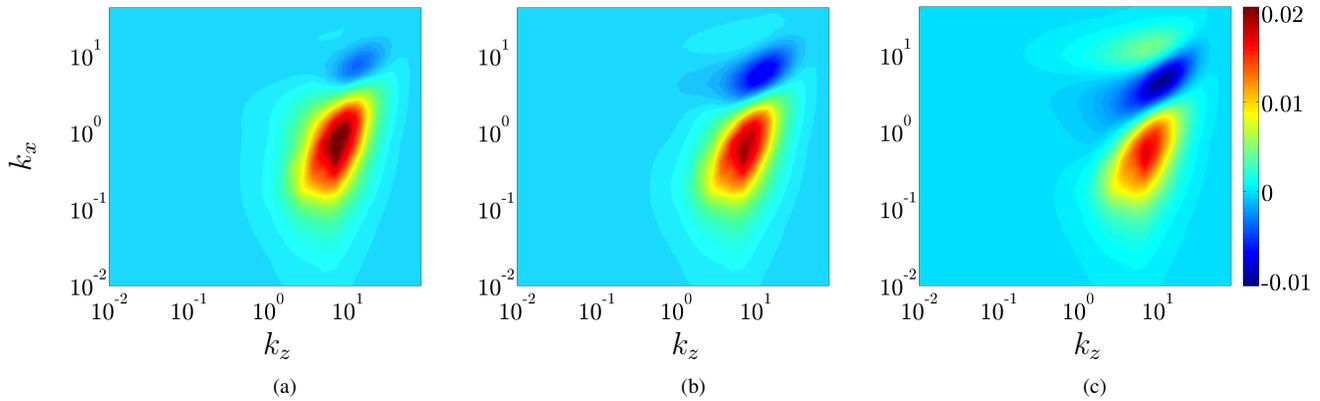
Fig. 5. Corrections to the pre-multiplied energy spectrum of velocity fluctuations induced by polymers, $\mathcal{E}_p(k_x, k_z) = k_x k_z E_p(k_x, k_z)$, for $R_\tau = 186$, $\beta = 0.9$, and $D_0 = 3.25$: (a) $We_\tau = 50$; (b) $We_\tau = 70$; and (c) $We_\tau = 100$. Perturbation series up to fifth order in α is used with Shanks approximation. All figures are shown in log-log-lin scale.

around the turbulent mean flow with polymers on drag reduction. The predicted turbulent mean velocity and drag reduction trends agree with previously reported simulation results. Furthermore, we have identified spatial length scales of fluctuations that are most amplified by stochastic disturbances.

Our results illustrate the predictive power of our model-based method and set the stage for studying the physical mechanisms responsible for the onset of drag reduction and the maximum drag reduction asymptote. Our ongoing effort is dedicated to identifying the underlying physics in high Weissenberg number regime.

REFERENCES

[1] C. M. White and M. G. Mungal, "Mechanics and prediction of turbulent drag reduction with polymer additives," *Annu. Rev. Fluid Mech.*, vol. 40, pp. 235–256, 2008.

[2] C. D. Dimitropoulos, R. Sureshkumar, and A. N. Beris, "Direct numerical simulation of viscoelastic turbulent channel flow exhibiting drag reduction: effect of the variation of rheological parameters," *J. Non-Newtonian Fluid Mech.*, vol. 79, pp. 433 – 468, 1998.

[3] T. Min, J. Y. Yoo, H. Choi, and D. D. Joseph, "Drag reduction by polymer additives in a turbulent channel flow," *J. Fluid Mech.*, vol. 486, pp. 213 – 238, 2003.

[4] C. F. Li, V. K. Gupta, R. Sureshkumar, and B. Khomami, "Turbulent channel flow of dilute polymeric solutions: Drag reduction scaling and an eddy viscosity model," *J. Non-Newtonian Fluid Mech.*, vol. 139, pp. 177–189, 2006.

[5] Y. Dubief, C. M. White, V. E. Terrapon, E. S. G. Shaqfeh, P. Moin, and S. K. Lele, "On the coherent drag-reducing and turbulence-enhancing behaviour of polymers in wall flows," *J. Fluid Mech.*, vol. 514, pp. 271–280, 2004.

[6] R. Moarref and M. R. Jovanović, "Controlling the onset of turbulence by streamwise traveling waves. Part 1: Receptivity analysis," *J. Fluid Mech.*, vol. 663, pp. 70–99, November 2010.

[7] B. K. Lieu, R. Moarref, and M. R. Jovanović, "Controlling the onset of turbulence by streamwise traveling waves. Part 2: Direct numerical simulations," *J. Fluid Mech.*, vol. 663, pp. 100–119, November 2010.

[8] R. Moarref and M. R. Jovanović, "Model-based design of transverse wall oscillations for turbulent drag reduction," *J. Fluid Mech.*, vol. 707, pp. 205 – 240, 2012.

[9] R. Sureshkumar and A. N. Beris, "Effect of artificial stress diffusivity on the stability of numerical calculations and the flow dynamics of time-dependent viscoelastic flows," *J. Non-Newtonian Fluid Mech.*, vol. 60, pp. 53 – 80, 1995.

[10] W. D. McComb, *The Physics of Fluid Turbulence*. Oxford University Press, 1991.

[11] W. C. Reynolds and W. G. Tiederman, "Stability of turbulent channel flow with application to malkus's theory," *J. Fluid Mech.*, vol. 27, no. 2, pp. 253–272, 1967.

[12] J. C. Del Alamo and J. Jiménez, "Spectra of the very large anisotropic scales in turbulent channels," *Phys. Fluids*, vol. 15, no. 6, pp. 41–44, 2003.

[13] K. D. Housiadas and A. N. Beris, "An efficient fully implicit spectral scheme for DNS of turbulent viscoelastic channel flow," *J. Non-Newtonian Fluid Mech.*, vol. 122, pp. 243 – 262, 2004.

[14] R. Sureshkumar, A. N. Beris, and R. A. Handler, "Direct numerical simulation of the turbulent channel flow of a polymer solution," *Phys. Fluids*, vol. 9, p. 743, 1997.

[15] M. R. Jovanović and T. T. Georgiou, "Reproducing second order statistics of turbulent flows using linearized navier-stokes equations with forcing," *Bulletin of the American Physical Society*, vol. 55, 2010.

[16] M. R. Jovanović and B. Bamieh, "Componentwise energy amplification in channel flows," *J. Fluid Mech.*, vol. 534, pp. 145–183, July 2005.

[17] D. Shanks, "Nonlinear transformations of divergent and slowly convergent sequences," *J. Math. Phys.*, vol. 34, pp. 1 – 42, 1955.

[18] J. A. C. Weideman and S. C. Reddy, "A MATLAB differentiation matrix suite," *ACM T. Math. Software*, vol. 26, no. 4, pp. 465–519, 2000.

[19] L. N. Trefethen, N. Hale, R. B. Platte, T. A. Driscoll, and R. Pachón, "Chebfun version 4," University of Oxford, 2011, http://www.maths.ox.ac.uk/chebfun/.

[20] G. Iaccarino, E. S. G. Shaqfeh, and Y. Dubief, "Reynolds-averaged modeling of polymer drag reduction in turbulent flows," *J. Non-Newtonian Fluid Mech.*, vol. 165, pp. 376–384, 2010.